Structure, Vibrational Absorption and Circular Dichroism Spectra, and Absolute Configuration of Tröger's Base

A. Aamouche, F. J. Devlin, and P. J. Stephens*

Contribution from the Department of Chemistry, University of Southern California, Los Angeles, California 90089-0482

Received October 13, 1999

Abstract: The structure of Tröger's Base, **1**, a heterocyclic amine containing two stereogenic N atoms, is predicted from ab initio Density Functional Theory (DFT), using the B3PW91 and B3LYP functionals and the 6-31G* basis set. Vibrational unpolarized absorption and vibrational circular dichroism (VCD) spectra are predicted thence. In the case of VCD, Atomic Axial Tensors (AATs) are calculated using Gauge-Invariant Atomic Orbitals (GIAOs). The predicted structure is in excellent agreement with the X-ray structure of **1**. The predicted vibrational spectra are in excellent agreement with experimental spectra of CCl_4 and CS_2 solutions of **1**, supporting the identicalness of the crystalline and solution conformations of **1**. No evidence of additional conformations of **1** in solution is found. The VCD spectra require the assignment of the (*R*,*R*)/(*S*,*S*) absolute configuration to (−)/(+)-**1**, opposite to that obtained from the electronic circular dichroism spectrum by Mason et al. and in accord with that obtained from X-ray crystallography of a salt of **1** containing monoprotonated **1**, **2**, and a chiral anion by Wilen et al. The structure of **2** predicted by DFT is also in excellent agreement with the X-ray structure.

Introduction

Tröger's Base,[1] **1**, is a chiral heterocyclic amine containing two stereogenic N atoms:

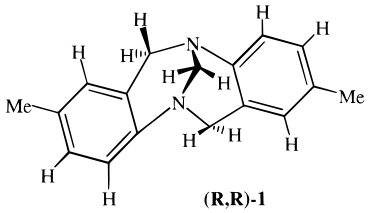

Resolution of **1** was reported in 1944 by Prelog and Wieland.[2] The absolute configuration of (+)-**1** was determined to be (*R*,*R*) by Mason et al. in 1967[3] from its near-ultraviolet electronic circular dichroism (CD), using the "Coupled Oscillator" (CO) or "Exciton Coupling" methodology.[4,5] The X-ray structure of racemic **1** was reported by Wilcox/Larson and Wilcox in 1985/1986.[6,7] In 1991, the X-ray structure of a salt, containing monoprotonated (+)-**1**, **2**, and the monoanion, **3**, of (−)-1,1′-binaphthalene-2,2′-diyl hydrogen phosphate, **4**, was reported by Wilen et al.[8] Given the *R* absolute configuration of (−)-**4**, the (*S*,*S*) absolute configuration was deduced for (+)-**1**, opposite to that reported earlier by Mason et al.[3]

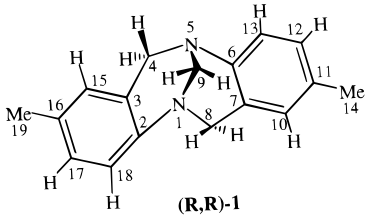

Figure 1. Atom numbering of **1**.

We report a study of the structure and absolute configuration of **1** using ab initio vibrational spectroscopy. The structure,

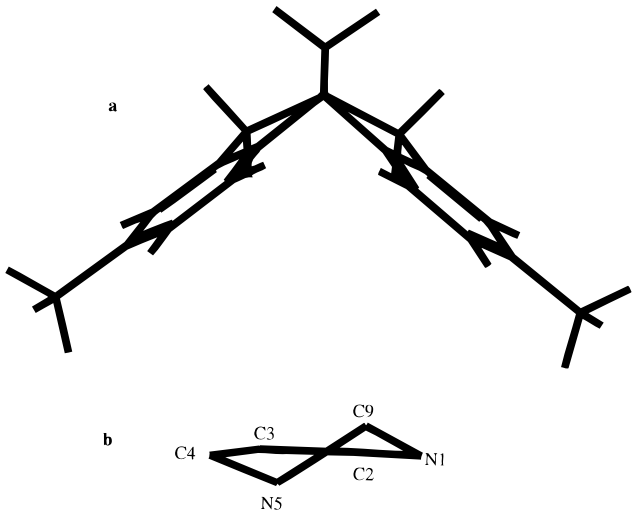

Figure 2. The B3PW91/6-31G* structure of (*R*,*R*)-**1**. (a) The entire molecule, as viewed with N1C9 and N5C9 eclipsed. (b) The N1C2C3C4N5C9 ring conformation.

* To whom correspondence should be addressed: stephens@chem1.usc.edu.

(1) Tröger, J. *J. Prakt. Chem.* **1887**, *36*, 225.
(2) Prelog, V.; Wieland, P. *Helv. Chim. Acta* **1944**, *27*, 1127.
(3) Mason, S. F.; Vane, G. W.; Schofield, K.; Wells, R. J.; Whitehurst, J. S. *J. Chem. Soc. B* **1967**, 553.
(4) Charney, E. *The Molecular Basis of Optical Activity: Optical Rotatory Dispersion and Circular Dichroism*, Wiley: **1979**, Chapter 4, p 110.
(5) Harada, N.; Nakanishi, K. *Circular Dichroic Spectroscopy: Exciton Coupling in Organic Stereochemistry*; University Science Books: Mill Valley, CA, 1983.
(6) Wilcox, C. S. *Tetrahedron Lett.* **1985**, *26*, 5749.
(7) Larson, S. B.; Wilcox, C. S. *Acta Crystallogr. Sect. C* **1986**, *C42*, 224.
(8) Wilen, S. H.; Qi, J. Z.; Williard, P. G. *J. Org. Chem.* **1991**, *56*, 485.

10.1021/ja993678r CCC: $19.00
Published on Web 02/29/2000

Table 1. Frequencies, Dipole Strengths, and Rotational Strengths of **1**[a]

	expt			B3PW91			B3LYP		
mode[b]	ν	D	R	ν	D	R	ν	D	R
87	1620	1.3	3.0	1686	0.6	8.3	1674	0.4	6.2
86	1616	1.4	−8.9	1685	12.5	−20.2	1672	10.8	−17.3
85	1578	2.0	−2.4	1639	2.6	−10.1	1626	2.1	−9.4
84	1575	0.8	3.6	1636	14.2	8.7	1624	12.7	9.1
83	1497	225.6	300.7	1553	133.0	148.0	1548	120.0	120.9
82	1492	312.2	−360.8	1548	362.7	−191.9	1543	316.1	−150.0
81	1478	16.3	2.1	1525	2.0	14.4	1530	0.6	6.2
80	1462	13.0	−5.9	1523	53.6	−43.3	1527	52.8	−46.2
79	1458	28.0	−40.4	1517	2.5	−10.6	1524	0.0	0.7
78	1443	7.1	−27.8	1510	13.6	3.6	1515	8.4	7.1
77	1440	4.2	13.1	1510	16.8	−2.1	1515	16.0	−6.0
76	1439	50.2	14.7	1500	29.1	8.0	1507	29.4	3.7
75	1435	7.7	−0.5	1497	3.7	−1.2	1505	2.2	−1.5
74	1415	5.2	−21.3	1466	8.1	−4.2	1462	8.1	−2.2
73	1412	65.4	−10.5	1462	90.2	−20.6	1458	85.5	−23.5
72	1378	1.5	0.2	1436	0.1	0.2	1444	0.2	−0.2
71	1376	11.1	6.0	1436	4.0	0.2	1443	10.1	−0.6
70	1360	14.7	−2.8	1407	22.9	−5.2	1410	35.6	−7.3
69	1345	33.6	81.3	1400	23.1	43.1	1391	22.0	40.5
68	1326	111.3	0.8	1383	100.2	2.7	1375	119.7	19.7
67	1324	42.1	−17.3	1376	0.4	−4.3	1372	5.5	−16.4
66	1301	23.0	−14.9	1359	94.4	−36.2	1347	58.6	−54.3
65	1297	23.8	−53.3	1353	10.7	−10.4	1342	5.6	−3.4
64	1291	36.8	−98.0	1337	38.3	−80.6	1333	32.0	−64.2
63	1265	6.3	−5.2	1306	4.9	−5.5	1306	1.4	0.2
62	1259	16.0	−20.2	1300	2.2	−1.8	1301	4.1	−4.4
61	1250	8.1	−15.9	1291	8.4	−5.4	1286	10.6	−11.9
60	1240	9.6	16.5	1274	0.4	2.9	1265	4.9	8.6
59	1225	18.2	−12.5	1263	8.0	−14.2	1257	6.6	−8.2
58	1206	230.7	66.0	1249	299.6	70.6	1242	337.8	34.9
57	1192	54.0	100.8	1230	32.5	84.5	1225	36.3	89.6
56	1164	17.0	18.4	1199	21.3	−0.7	1193	16.0	−1.5
55	1148	14.0	−32.4	1183	7.4	−16.1	1181	2.6	−10.0
54	1142	36.1	12.9	1177	34.4	6.9	1177	26.0	3.7
53	1114	90.6	101.5	1145	102.5	33.7	1139	99.8	64.5
52	1099	58.6	−40.8	1135	0.1	3.2	1122	8.6	−31.5
51	1094	31.8	−52.3	1134	67.9	−42.5	1122	60.8	−39.9
50	1066	86.5	−29.0	1094	37.0	−13.0	1091	49.8	0.2
49	1044	11.1	−9.8	1069	10.8	−2.0	1075	7.3	−1.7
48	1038	18.1	−8.9	1069	35.4	−7.5	1075	28.9	−10.5
47	1018	4.1	−14.1	1040	2.2	−4.9	1038	2.8	−10.4
46	997	9.4	−72.3	1031	1.3	11.5	1033	3.7	19.3
45	990	10.4	−62.6	1026	27.2	−85.3	1027	28.7	−79.3
44	970	39.5	69.3	994	77.9	94.3	993	57.5	71.6
43	964	105.8	104.2	989	77.8	55.5	983	88.7	56.6
42	951	170.8	−70.2	977	237.0	−114.7	967	255.5	−98.2
41	943	60.7	−44.3	957	1.0	−2.2	957	1.0	−1.8
40	939	13.2	10.1	957	1.7	2.2	956	0.4	1.8
39	919	2.1	−2.2	940	0.6	−3.4	935	0.3	−2.0
38	899	118.9	−101.5	924	94.7	−48.1	915	131.3	−56.0
37	873	9.5	5.9	891	3.4	2.1	894	2.8	0.9
36	870	36.3	7.8	889	11.7	14.2	892	10.7	15.6
35	832	247.8	−91.0	846	233.4	−127.0	847	196.8	−101.4
34	824	117.0	26.4	841	74.6	12.6	843	62.7	5.0
33[c]	806	25.0	22.2	823	5.4	−14.7	822	12.4	−25.7
32[c]	748	29.3	36.3	760	35.9	5.7	759	31.3	7.2
31[c]	739	36.4	0.9	757	6.2	0.6	755	6.7	1.3
30[c]	730	4.0	14.8	745	1.0	2.1	744	0.0	0.0
29	721	3.5		740	1.7	−6.0	738	3.3	−6.9
28	715	27.0		731	21.4	−22.8	731	21.9	−20.3
27	691	16.9		704	6.3	−1.2	699	7.9	−1.8
26	636	128.5		644	73.2	2.2	644	74.9	1.3
25	584	104.0		595	50.6	−1.1	597	45.5	−0.7
24	570	62.6		580	20.6	33.8	582	15.7	28.4
23	561	33.9		572	10.3	−15.8	573	6.5	−12.0
22	529	43.3		532	21.6	−4.5	535	22.2	−4.6
21	511	43.7		518	35.0	−8.2	519	31.0	−5.7
20	476	5.2		482	2.4	−1.1	484	2.8	−1.0
19	470	25.7		475	18.6	−20.8	477	15.7	−17.4
18	456	27.7		462	7.7	−1.6	464	8.2	−1.5
17	431	24.0		434	8.9	−6.3	435	6.2	−6.1
16	423	32.4		430	6.7	5.9	432	5.2	5.2
15	411	81.4		413	37.2	46.6	414	31.6	42.6
14	384	22.2		389	23.8	−3.3	391	18.3	−3.6

[a] Frequencies in cm^{-1}; dipole strengths in 10^{-40} esu^2 cm^2; rotational strengths in 10^{-44} esu^2 cm^2. Calculated and experimental rotational strengths are for (*R*,*R*)-**1** and (−)-**1**, respectively. [b] From Lorentzian fitting of CCl_4 spectra, except where indicated.We report parameters only for bands assigned to fundamentals. Additional bands included in the fits at 1126, 1216, 1514, and 1525 cm^{-1} are assigned to nonfundamentals or to impurities. [c] From CS_2 spectra.

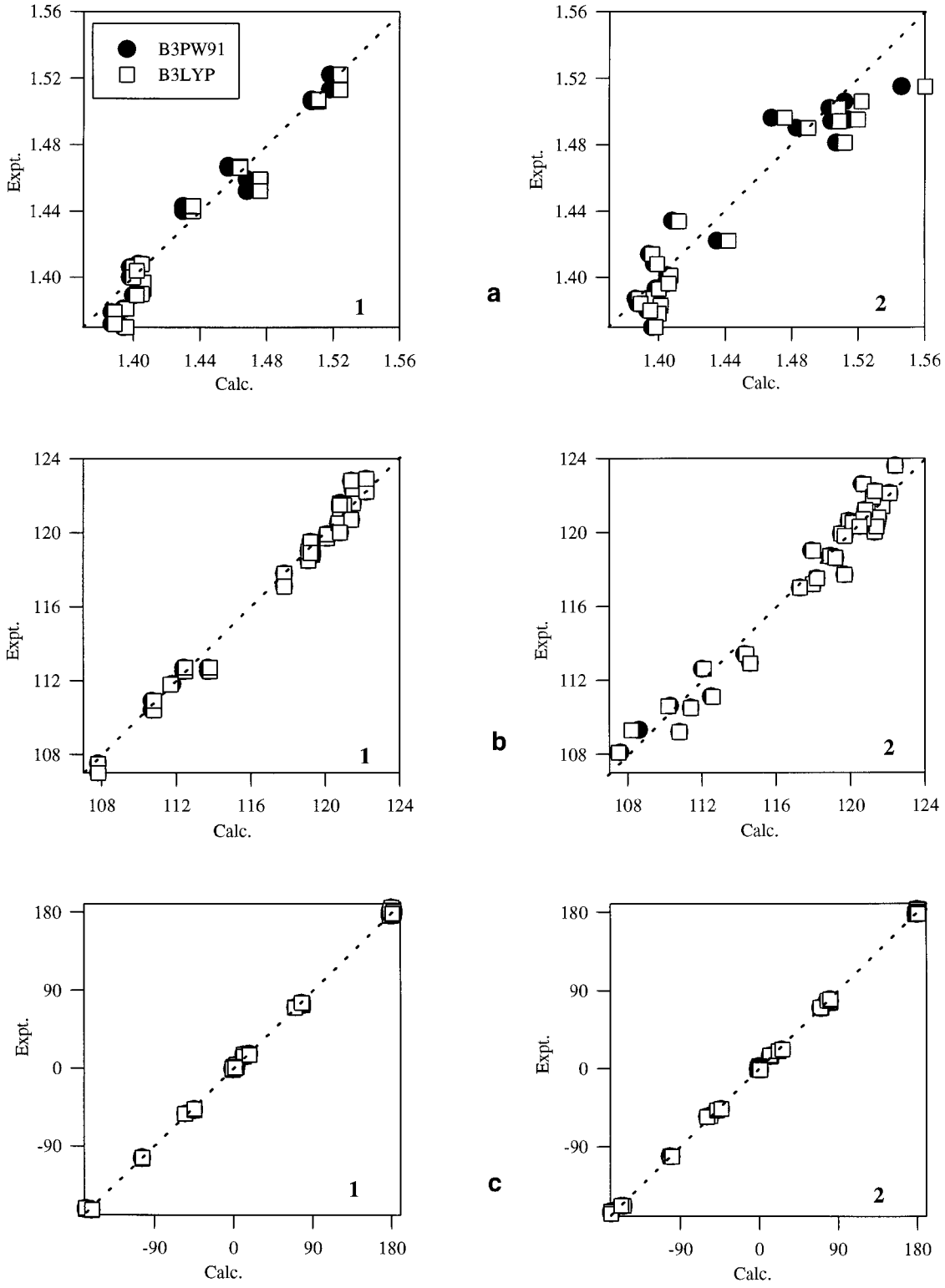

Figure 3. Comparison of calculated and experimental structural parameters of **1** and **2**: (a) bond lengths; (b) bond angles; and (c) dihedral angles. The slopes of the lines are +1.

vibrational unpolarized absorption spectrum, and vibrational circular dichroism (VCD)[9] spectrum of **1** are predicted using ab initio Density Functional Theory (DFT).[10] The predicted structure is in excellent agreement with the X-ray structure.[6,7] The predicted vibrational spectra are in excellent agreement with the experimental spectra in solution in CCl_4 and CS_2. Comparison of predicted and observed VCD spectra confirms the (*S*,*S*)-(+)/(*R*,*R*)-(−) absolute configuration of **1**. In addition, we have predicted the structure of monoprotonated **1**, **2**. The agreement with the experimental structure is excellent.

Our work takes advantage of the recent development and implementation of analytical derivative techniques for the

(9) (a) Stephens, P. J.; Lowe, M. A. *Annu. Rev. Phys. Chem.* **1985**, *36*, 213; (b) Nafie, L. A. *Annu. Rev. Phys. Chem.* **1997**, *48*, 357.

(10) *Chemical Applications of Density Functional Theory*, Laird, B. B., Ross, R. B., Ziegler, T., Eds.; ACS Symposium Series 629; American Chemical Society: Washington, D. C., 1996.

calculation of DFT Atomic Axial Tensors (AATs) using Gauge-Invariant Atomic Orbitals (GIAOs)[11] which, together with DFT harmonic force fields (HFFs) and Atomic Polar Tensors (APTs), permit the prediction of vibrational rotational strengths and VCD spectra.[12] This theoretical methodology has previously been applied to a number of chiral molecules, including *trans*-2,3d_2-oxirane,[11] 6,8-dioxabicyclo[3.2.1]octane[13] and several mono- and dimethyl derivatives,[14] camphor,[15] fenchone,[15] α-pinene,[16] phenyloxirane,[17] cyclohexanone-2d_1 and -*trans*-2,6d_2,[18] and 3-methylcyclohexanone.[19]

Methods

(+)-, (−)-, and (±)-**1** were obtained from Aldrich and (−)-**1** from Fluka and used without further purification. Specified chemical purities were: (+), >99%; (−), >99%; (±), 98% (Aldrich); (−), 99% (Fluka). Specified specific rotations were: (+), $[\alpha]^{20}_D = +280°$ ($c = 0.5$, hexane); (−), $[\alpha]^{20}_D = -280°$ ($c = 0.5$, hexane) (Aldrich) and −283° ($c = 0.3$, hexane) (Fluka). Prior literature values for (+)-**1** are: $[\alpha]^{17}_D = 287 \pm 7°$ ($c = 0.281$, hexane)[2]; $[\alpha]^{25}_D = 287 \pm 2°$ ($c = 0.29$, hexane).[8] The latter value was obtained on (+)-**1** whose enantiomeric purity was >99%.[8] Aldrich and Fluka (+)- and (−)-**1** can therefore be assumed to possess enantiomeric excess (ee) > 95%.

Vibrational unpolarized absorption spectra of CCl_4 and CS_2 solutions of **1** were obtained using a Nicolet MX-1 spectrometer at 1 cm^{-1} resolution. VCD spectra of CCl_4 and CS_2 solutions of **1** were obtained using Bomem/BioTools Chiral*IR* spectrometers at 4 cm^{-1} resolution. All experiments used a variable-path cell (Graseby Specac Ltd., UK) with KBr windows. Frequencies, dipole strengths, and rotational strengths were obtained from experimental absorption and VCD spectra via Lorentzian fitting.[15b,16]

DFT calculations were carried out using the Gaussian program[20] as described previously.[11,13−19] The hybrid density functionals B3PW91[21] and B3LYP[22] were used together with the 6-31G* [23] basis set (321 basis functions). All calculations used direct, analytical derivative methods. Atomic Axial Tensors (AATs) were calculated using GIAOs; as a result, Common Origin gauge[12,24] vibrational rotational strengths are origin-independent. Absorption and VCD spectra were synthesized from calculated vibrational frequencies, dipole strengths, and rotational strengths, assuming Lorentzian band shapes.

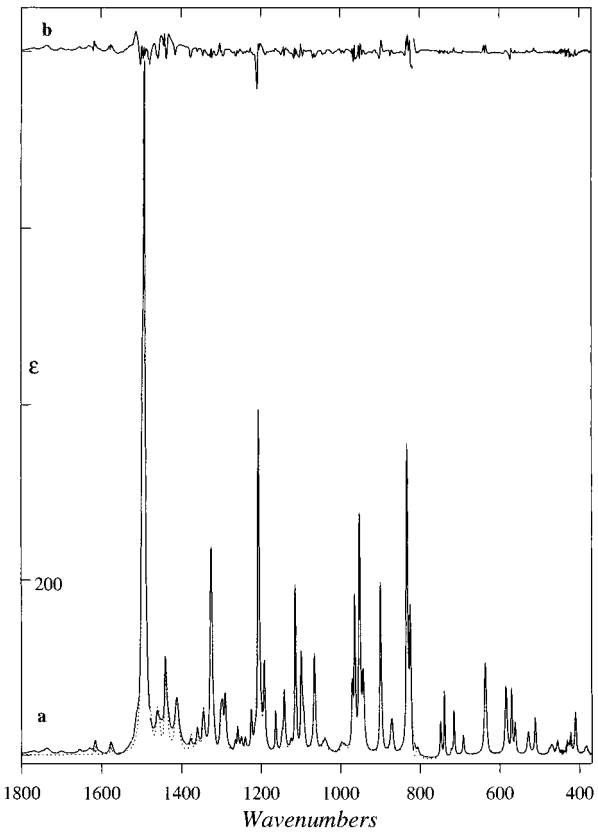

Figure 4. Mid-IR absorption spectrum of **1**. (a) Solid line: experimental spectrum of **1** in CCl_4 (0.2 M (±)-**1**; 370−730, 815−1480, and 1525−1800 cm^{-1}; 0.1 M (−)-**1**; 1480−1525 cm^{-1}) and in CS_2 (0.2 M (−)-**1**; 730−815 cm^{-1}). Resolution is 1 cm^{-1}. Dotted line: Lorentzian fit. (b) The difference between the experimental spectrum and Lorentzian fit.

Results

Equilibrium structures of **1** have been calculated at the B3PW91/6-31G* and B3LYP/6-31G* levels. Bond lengths, bond angles, and dihedral angles of the two structures are given in Table 1 of the Supporting Information. The atom numbering is detailed in Figure 1. The structures exhibit C_2 symmetry. B3PW91 and B3LYP structures are qualitatively identical. The B3PW91 structure is illustrated in Figure 2a. The N1C2C3C4C15-C16C19C17C18 and N5C6C7C8C10C11C14C12C13 moieties are very nearly planar. The N1C2C3C4N5C6C7C8 ring is boatlike. A rigid conformation is enforced by the CH_2 bridge. The conformation of the C_4N_2 rings is shown in Figure 2b.

Quantitatively, we note that B3LYP bond lengths are systematically longer than B3PW91 bond lengths, the difference varying from 0.002 to 0.008 Å; the largest differences are for bonds in the C_4N_2 rings. Bond angles and dihedral angles differ very little; maximum differences are 0.1 and 0.5°, respectively.

(11) Cheeseman, J. R.; Frisch, M. J.; Devlin, F. J.; Stephens, P. J. *Chem. Phys. Lett.* **1996**, *252*, 211.
(12) (a) Stephens, P. J. *J. Phys. Chem.* **1985**, *89*, 748; (b) Stephens, P. J. *J. Phys. Chem.* **1987**, *91*, 1712.
(13) Stephens, P. J.; Cheeseman, J. R.; Frisch, M. J.; Ashvar, C. S.; Devlin, F. J. *Mol. Phys.* **1996**, *89*, 579.
(14) (a) Ashvar, C. S.; Stephens, P. J.; Eggimann, T.; Wieser, H. *Tetrahedron: Asymmetry* **1998**, *9*, 1107. (b) Ashvar, C. S.; Devlin, F. J.; Stephens, P. J.; Bak, K. L.; Eggimann, T.; Wieser, H. *J. Phys. Chem. A* **1998**, *102*, 6842.
(15) (a) Devlin, F. J.; Stephens, P. J.; Cheeseman, J. R.; Frisch, M. J. *J. Am. Chem. Soc.* **1996**, *118*, 6327; (b) Devlin, F. J.; Stephens, P. J.; Cheeseman, J. R.; Frisch, M. J. *J. Phys. Chem.* **1997**, *101*, 6322.
(16) Devlin, F. J.; Stephens, P. J.; Cheeseman, J. R. Frisch, M. J. *J. Phys. Chem.* **1997**, *101*, 9912.
(17) Ashvar, C. S.; Devlin, F. J.; Stephens, P. J. *J. Am. Chem. Soc.* **1999**, *121*, 2836.
(18) Devlin, F. J.; Stephens, P. J. *J. Phys. Chem. A* **1999**, *103*, 527.
(19) Devlin, F. J.; Stephens, P. J. *J. Am. Chem. Soc.* **1999**, *121*, 7413.
(20) *GAUSSIAN 95*, Development version, and *GAUSSIAN 98*; Frisch, M. J.; Trucks, G. W.; Schlegel, H. B.; Scuseria, G. E.; Robb, M. A.; Cheeseman, J. R.; Zakrzewski, V. G.; Montgomery, J. A., Jr.; Stratmann, R. E.; Burant, J. C.; Dapprich, S.; Millam, J. M.; Daniels, A. D.; Kudin, K. N.; Strain, M. C.; Farkas, O.; Tomasi, J.; Barone, V.; Cossi, M.; Cammi, R.; Mennucci, B.; Pomelli, C.; Adamo, C.; Clifford, S.; Ochterski, J.; Petersson, G. A.; Ayala, P. Y.; Cui, Q.; Morokuma, K.; Malick, D. K.; Rabuck, A. D.; Raghavachari, K.; Foresman, J. B.; Cioslowski, J.; Ortiz, J. V.; Stefanov, B. B.; Liu, G.; Liashenko, A.; Piskorz, P.; Komaromi, I.; Gomperts, R.; Martin, R. L.; Fox, D. J.; Keith, T.; Al-Laham, M. A. Peng, C. Y.; Nanayakkara, A.; Gonzalez, C.; Challacombe, M.; Gill, P. M. W.; Johnson, B.; Chen, W.; Wong, M. W.; Andres, J. L.; Head-Gordon, M.; Replogle, E. S.; Pople, J. A. Gaussian, Inc.: Pittsburgh, PA, 1998.
(21) Becke, A. D. *J. Chem. Phys.* **1993**, *98*, 1372, 5648.
(22) Stephens, P. J.; Devlin, F. J.; Chabalowski, C. F.; Frisch, M. J. *J. Phys. Chem.* **1994**, *98*, 11623.
(23) Hehre, W. J.; Schleyer, P. R.; Radom, L.; Pople, J. A. *Ab Initio Molecular Orbital Theory*, Wiley: New York, 1986.
(24) Stephens, P. J.; Jalkanen, K. J.; Amos, R. D.; Lazzeretti, P.; Zanasi, R. *J. Phys. Chem.* **1990**, *94*, 1811.

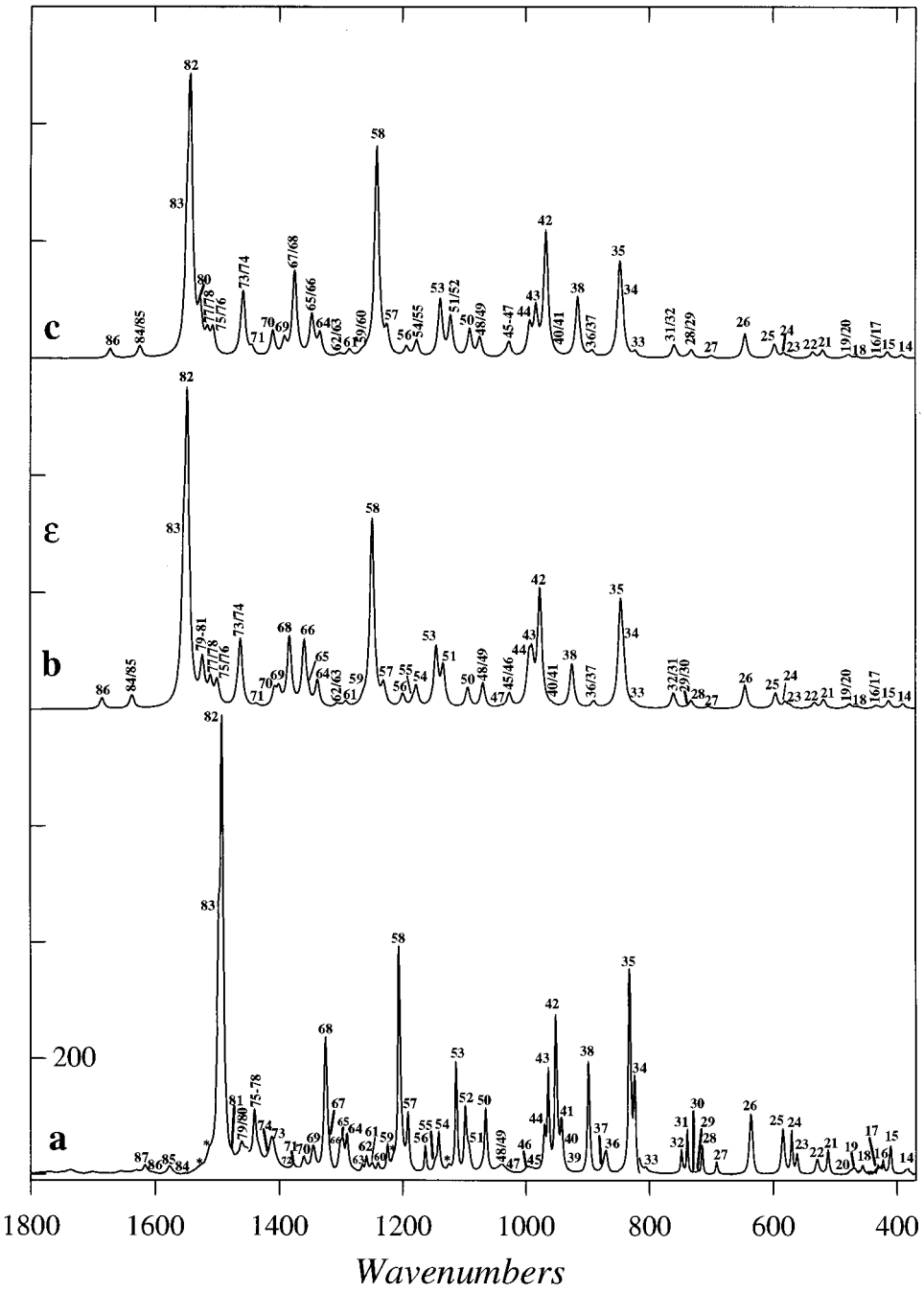

Figure 5. Mid-IR absorption spectrum of **1**. (a) Experimental spectrum (from Figure 4); (b) B3PW91/6-31G* spectrum; (c) B3LYP/6-31G* spectrum. Lorentzian band shapes are used ($\gamma = 4.0$ cm^{-1}). Fundamentals are numbered. Asterisks denote bands not assigned as fundamentals of **1**.

The maximum deviation from 0° of the dihedral angles of the C atoms of the phenyl rings is 1.0° for C10C11C12C13/C15C16C17C18. The B3PW91/B3LYP dihedral angles C8C7-C6C13/C4C3C2C18 and C8C7C10C11/C4C3C15C16 deviate from 180° by 2.5/2.2 and 2.3/2.0°, respectively. N1/N5 and C9 are on opposite sides of the N5C6C7C8/N1C2C3C4 planes, respectively. The B3PW91/B3LYP dihedral angles N5C4C3C2/N1C8C7C6 and C3C2N1C9/C7C6N5C9 are 11.0/11.0 and 17.5/18.0°, respectively.

The methyl groups substituted on the phenyl rings adopt conformations in which one C−H is very nearly coplanar with the adjacent phenyl ring. In the case of the methyl group substituted at C11/C16, this H is cis with respect to C10/C15. We have examined the variation in energy of **1** on rotation of the two methyl groups (maintaining C_2 symmetry), at the B3PW91/6-31G* level. The barrier is 3-fold. Rotation by 180° does not lead to a second minimum. Thus, no other inequivalent conformations of the methyl groups are predicted.

Equilibrium structures have also been calculated for **2** at the B3PW91/6-31G* and B3LYP/6-31G* levels. Bond lengths, bond angles, and dihedral angles are given in Table 1 of the Supporting Information. Large changes in bond lengths on protonation of **1** occur only for the N1C2, N1C8, N1C9, and N5C9 bonds. The B3PW91/B3LYP changes are 0.053/0.054 Å, 0.044/0.046 Å, 0.089/0.096 Å, and −0.049/−0.052 Å, respectively. All other bond length changes are ≤0.012 Å. The largest changes in bond angles occur for C4N5C9, N5C9N1, and C18C2C3. The B3PW91/B3LYP changes are 3.0/3.0°, −3.2/−3.5°, and 2.9/2.9°, respectively. All other changes are <2.0°. Surprisingly, the bond angles C2N1C8, C2N1C9, and C8N1C9 change very little. The B3PW91/B3LYP changes are 0.6/0.6°, −0.4/−0.6°, and −0.2/−0.3°, respectively. The largest

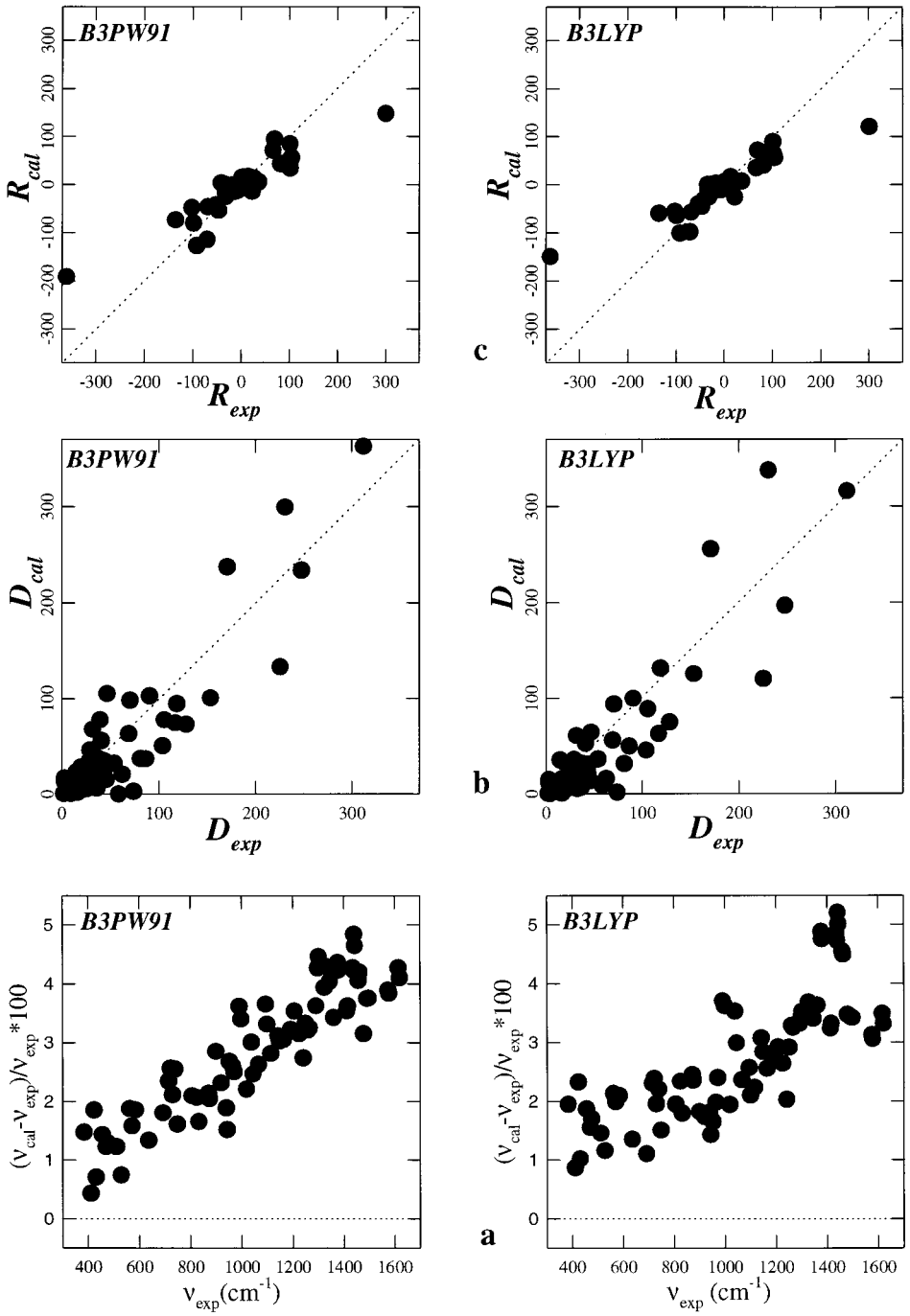

Figure 6. Comparison of calculated and experimental frequencies, dipole strengths, and rotational strengths of **1**. The slopes of the dotted lines in (b) and (c) are +1. Calculated and experimental rotational strengths are for (*R*,*R*)-**1** and (−)-**1**, respectively. Dipole and rotational strengths have been summed for the following unresolved bands: 36/37, 40/41, 45/46, 48/49, 65/66, 67/68, 71/72, 73/74, 75−78, 79/80, 84/85, and 86/87.

changes in dihedral angles occur for C4C3C2N1, C3C2N1C8, C3C2N1C9, C7C6N5C9, C6N5C9N1, C8C7C6N5, C18C2C3C4, and C13C6N5C9. The B3PW91/B3LYP changes are −5.0/−5.0°, 4.3/4.3°, 4.1/3.9°, 8.2/8.3°, −4.4/−4.3°, −4.5/−4.6°, −4.3/−4.3°, and 6.5/6.1°, respectively. All other changes are <4.0°.

Experimental bond lengths, bond angles, and dihedral angles obtained by X-ray crystallography for **1** and **2** are given in Table 1 of the Supporting Information. (Note that in the case of **1** there is more than one inequivalent molecule in the unit cell. We have selected one of these (G) in Table 1 of the Supporting Information. Its symmetry is lower than C_2. Differences in parameters which are identical in C_2 symmetry provide a gauge of the changes in molecular structure due to intermolecular forces.) A comparison of calculated and experimental parameters is presented graphically in Figure 3. Overall, the agreement of theory and experiment is excellent. B3PW91 and B3LYP calculations give very similar agreement. It is clear from Figure 3 that the agreement of calculated and experimental bond lengths and bond angles is qualitatively superior in the case of **1**, as compared with **2**. The poorer agreement in the case of **2** may be attributable to the greater magnitude of intermolecular interactions in the ionic salt {**2**,**3**} than in crystalline **1** (note, in particular, that **2** is hydrogen bonded to **3**). Quantitatively, the mean absolute deviations of the B3PW91/B3LYP and experimental bond lengths, bond angles, and dihedral angles in Table 1 are 0.009/0.009 Å, 0.5/0.5°, and 2.0/2.1°, respectively, for **1** and 0.014/0.016 Å, 0.8/0.8°, and 1.7/1.7°, respectively, for **2**.

The mid-IR absorption spectrum of **1** is shown in Figure 4. The spectrum has been measured for both CCl_4 and CS_2 solutions of **1**. In Figure 4, the CCl_4 solution spectrum is shown, except in the region of strong CCl_4 absorption, where the spectrum of the CS_2 solution is shown. Harmonic vibrational frequencies and dipole strengths predicted using the B3PW91 and B3LYP functionals at the 6-31G* basis set level are given in Table 1. Mid-IR absorption spectra predicted thence are shown in Figure 5, together with the experimental spectrum. The B3PW91 and B3LYP spectra are qualitatively very similar. Allowing for the expected shift to higher frequency of calculated spectra, relative to the experimental spectrum, attributable to both errors in the harmonic frequencies and anharmonicity,[25] assignment of the experimental spectrum is straightforward, as shown in Figure 6. Fundamentals 14−35, 38, 42−44, 50−64, 69, 70, and 81−83 are clearly resolved. Fundamentals 36/37, 40/41, 45/46, 48/49, 65/66, 67/68, 71/72, 73/74, 75−78, 79/80, 84/85, and 86/87 are not resolved. Fundamentals 39 and 47 are very weak. Four bands are clearly observed which cannot be assigned as fundamentals (asterisked in Figure 5). Overall, the predicted and experimental spectra are in excellent qualitative agreement.

Quantitative values of experimental frequencies and dipole strengths have been obtained by Lorentzian fitting of the experimental spectrum. The fit is shown in Figure 4. The parameters obtained are given in Table 1. Comparison to calculated frequencies and dipole strengths is shown in Figure 6. Calculated frequencies are uniformly greater than experimental frequencies, the percentage deviations lying in the range 0−6%. Percentage deviations generally increase with increasing frequency; the variation is slightly more regular in the case of the B3PW91 functional. Calculated and experimental dipole strengths correlate well for both functionals. The agreement of calculated frequencies and dipole strengths with experimental values strongly supports the assignments of fundamentals.

The mid-IR VCD spectrum of (−)-**1** is shown in Figure 7. The spectrum has been measured in CCl_4 and CS_2 solutions. In Figure 7, the CCl_4 spectrum is shown except in the region of strong CCl_4 absorption, where the spectrum of the CS_2 solution is shown. Harmonic rotational strengths predicted using the B3PW91 and B3LYP functionals and the 6-31G* basis set for (*R*,*R*)-**1** are given in Table 1. Mid-IR VCD spectra predicted thence are shown in Figure 8, together with the experimental spectrum. The B3PW91 and B3LYP spectra are qualitatively similar. The assignment of the experimental VCD spectrum follows from the assignment of the absorption spectrum, as shown in Figure 8. The predicted spectra are in excellent qualitative agreement with the experimental spectrum. Fundamentals 30, 32−35, 38, 39, 42−44, 47, 50, 53−64, 69, 70, 82, and 83 are clearly resolved; their signs are in agreement with theory, except for 33 and 56. Mode 33 is predicted to be weak and negative, while it is observed to be weak and positive. Mode 56 is predicted to be weak and negative, while it is medium in strength and positive. In the case of modes 50 and 63, B3PW91 and B3LYP predictions differ in magnitude and sign; the former are in agreement with experiment. Fundamentals 36/37, 40/41, 45/46, 48/49, 51/52, 65/66, 67/68, 71/72, 73/74, 75−78, 79/80, 84/85, and 86/87 are not resolved; their net signs are in agreement with theory. Fundamentals 31 and 81 are very weak.

Quantitative rotational strengths have been obtained by Lorentzian fitting of the experimental VCD spectrum. The fit is shown in Figure 7. The rotational strengths obtained are given in Table 1. A comparison of calculated and experimental rotational strengths is shown in Figure 5. The correlation is excellent, further supporting the assignment of fundamentals.

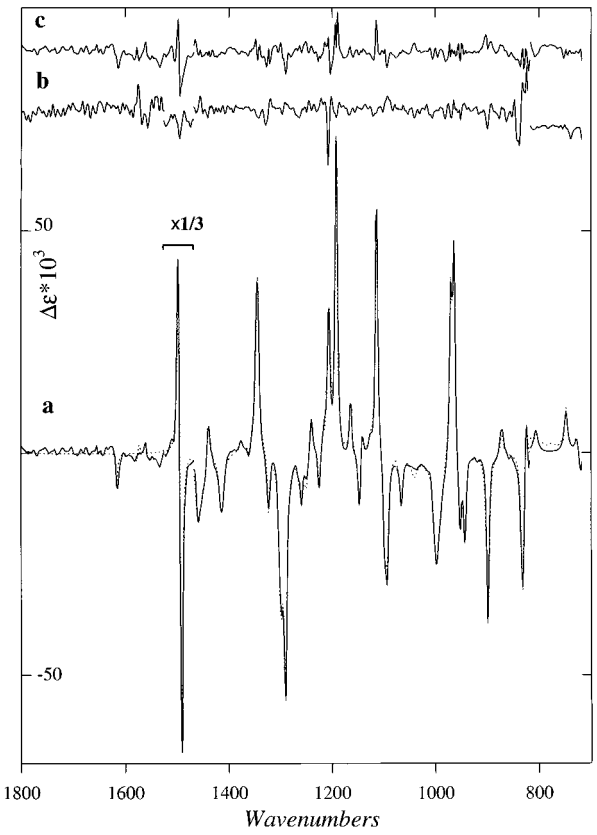

Figure 7. Mid-IR VCD spectrum of (−)-**1**. (a) Solid line: experimental spectrum in CCl_4 solution (0.2 M; 815−1470 and 1525−1800 cm^{-1}; 0.1 M; 1470−1525 cm^{-1}) and in CS_2 solution (0.2 M; 715−815 cm^{-1}). The spectrum is the "half-difference" spectrum: $^1/_2\{[\Delta\epsilon(-) - \Delta\epsilon(\pm)] - [\Delta\epsilon(+) - \Delta\epsilon(\pm)]\}$. Resolution is 4 cm^{-1}. Scan time is 1 h. Dotted line: Lorentzian fit. (b) Experimental "half-sum" spectrum $^1/_2\{[\Delta\epsilon(-) - \Delta\epsilon(\pm)] + [\Delta\epsilon(+) - \Delta\epsilon(\pm)]\}$. This spectrum measures the deviation from exact-mirror-image behavior of the VCD spectra of (+)- and (−)-**1**, obtained using the spectrum of (±)-**1** as the baseline. It is nonzero due to (a) noise and (b) artifacts which are not identical in (+)-, (−)-, and (±)-**1**. It defines the level of reliability of the VCD spectrum. (c) The difference between the experimental spectrum and Lorentzian fit.

The excellent agreement of VCD intensities calculated for the (*R*,*R*) absolute configuration with experimental intensities for (−)-**1** unambiguously defines the absolute configuration of **1** as (*R*,*R*)-(−)/(*S*,*S*)-(+). This result is in agreement with that obtained by Wilen et al. from the X-ray structure of {**2**,**3**} by reference to the absolute configuration of **4** and opposite to that deduced by Mason et al. from the electronic CD spectrum of **1**.

Discussion

In their analysis of the electronic CD spectrum of **1**, Mason et al. hypothesized the possibility of two conformations of **1** (labeled **I**a and **I**b and referred to as folded and open, respectively) in which the N_2C_4 rings are twist and half-boat conformations, respectively (ref 3, structures **III**a and **III**b). They selected **I**a as the dominant conformation. Subsequently, X-ray crystallography demonstrated the presence of twist conformations of the N_2C_4 rings in crystalline **1**. In solution it is possible that (1) the conformation is the same as in the crystalline state and no other stable conformation is energetically accessible; (2) more than one conformation is accessible, that

(25) Finley, J. W.; Stephens, P. J. *THEOCHEM* **1995**, *357*, 225.

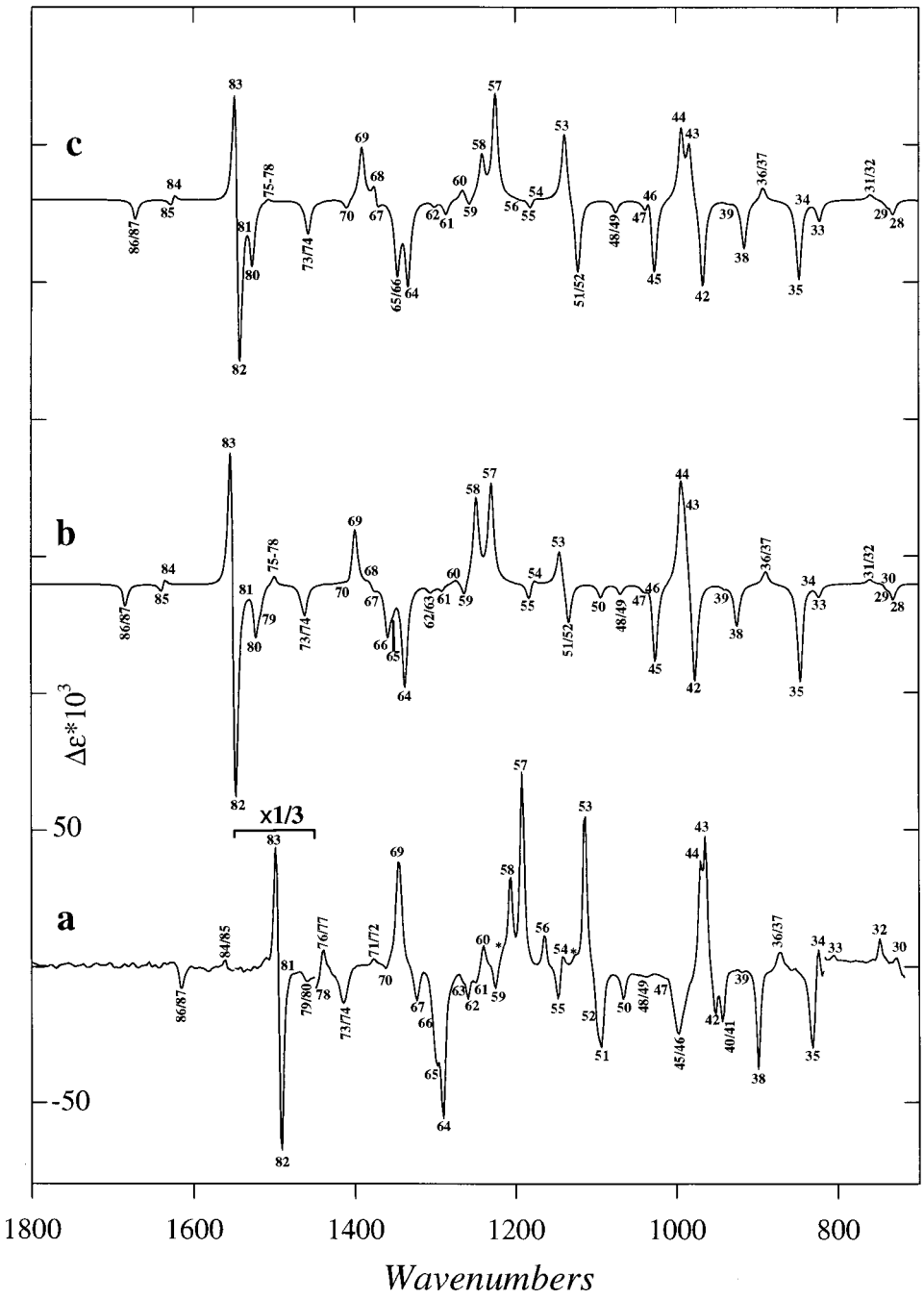

Figure 8. Mid-IR VCD spectra of **1**. (a) Experimental spectrum of (−)-**1** (from Figure 7); (b) B3PW91/6-31G* spectrum of (*R*,*R*)-**1**; (c) B3LYP/6-31G* spectrum of (*R*,*R*)-**1**. In (b) and (c), Lorentzian band shapes are used ($\gamma = 4.0$ cm^{-1}). Fundamentals are numbered.

found in the crystalline state being either the majority conformation or a minority conformation. Our results support the former situation. First, the B3PW91/6-31G* and B3LYP/6-31G* structures of **1** are qualitatively identical to the X-ray structure. We have been unable to locate additional minima on the potential energy surface of **1**. In particular, attempts to locate a stable structure containing half-boat N_2C_4 rings have not been successful. Second, the vibrational spectra predicted for **1** are in excellent agreement with the observed solution spectra, demonstrating that the calculated structure is indeed the solution structure. Very few bands are not assignable as fundamentals of **1**; as a result, the presence of a significant population of a second conformation in solution can be ruled out. Further support for the conclusion that **1** is a rigid molecule is provided by the identicality of the conformation of its monoprotonated cation, **2**, both as predicted by B3PW91/6-31G* and B3LYP/6-31G* calculations and as observed by X-ray crystallography.

The DFT structures of **1** are in excellent quantitative agreement with the X-ray structure. The differences in calculated and experimental bond lengths, bond angles and dihedral angles can be attributed to a combination of factors: (1) theoretical error, due to inadequacies of the functionals and basis set; (2) intermolecular interactions in crystalline **1**; (3) experimental error in the X-ray structure. None are large. The agreement of the calculated and experimental structures of **2** is somewhat poorer. It seems most likely that this is due to larger intermolecular effects in crystalline {**2**,**3**}, due to the ionic nature of **2** and **3**.

In comparing predicted and experimental VCD spectra of **1**, one can choose the spectrum predicted for either the (*R*,*R*) or

(*S*,*S*) absolute configuration and the experimental spectrum of either (+)- or (−)-**1**. In Figure 8, the predicted spectrum is for the (*R*,*R*) absolute configuration and the experimental spectrum is for the (−) enantiomer. The excellent qualitative and quantitative agreement of these predicted and experimental spectra unambiguously establishes the absolute configuration of **1** as (*R*,*R*)-(−)/(*S*,*S*)-(+). The absolute configuration of **1** was first determined by Mason et al. using electronic CD. The rotational strengths of the $\pi \rightarrow \pi^*$ transitions originating in the phenyl rings were calculated using the CO model. Assignment of the experimental CD spectrum led to the absolute configuration (*R*,*R*)-(+). The conformation of **1** assumed by Mason et al. is qualitatively identical to that of our DFT structure. Thus, it must be concluded that the erroneous absolute configuration deduced by Mason et al. results from inadequacies of the CO model calculation. Our absolute configuration of **1** is identical to that obtained by Wilen et al. from the X-ray structure of {**2**,**3**}, the validity of which rests on the reliability of the absolute configuration of **4**. In contrast, our methodology is direct and does not require the knowledge of the absolute configuration of any other molecule.

Conclusion

We have demonstrated the practical utility of VCD spectroscopy in combination with ab initio DFT in establishing the absolute configurations of chiral organic molecules. Tröger's Base contains 37 atoms. At this time, DFT-GIAO calculations can be easily carried out at the 6-31G* basis set level for much larger molecules. The applicability of the methodology is quite wide, therefore, and will, of course, increase with improvements in computer hardware and software. VCD spectroscopy should therefore constitute an attractive alternative to electronic CD spectroscopy and X-ray crystallography in future determinations of absolute configurations.

Acknowledgment. We are grateful to NIH (GM051972-04) and NSF (CHE-9902832) for support of this work, to Elf Aquitaine/Sanofi for a postdoctoral fellowship (to A. A.), and to Drs. M. J. Frisch and J. R. Cheeseman for discussions and assistance.

Supporting Information Available: A table of calculated and experimental structural parameters for **1** and **2** is included in the Supporting Information. This material is available free of charge via the Internet at http://pubs.acs.org.

JA993678R